Biosynthetic engineering and fermentation media development leads to gram-scale production of spliceostatin natural products in *Burkholderia* sp.

Alessandra S. Eustáquio[1,2]*, Li-Ping Chang[1], Greg L. Steele[1], Christopher J. O'Donnell[1], Frank E. Koehn[1]

[1]Natural Products Laboratory, Worldwide Medicinal Chemistry, Pfizer Worldwide Research and Development, 445 Eastern Point Road, Groton, Connecticut 06340, USA

[2]Present address: University of Illinois at Chicago, College of Pharmacy, Department of Medicinal Chemistry & Pharmacognosy and Center for Pharmaceutical Biotechnology, 900 S Ashland Avenue, Chicago, IL 60607, USA

***Corresponding author:** ase@uic.edu

Abstract

A key challenge in natural products drug discovery is compound supply. Hundreds of grams of purified material are needed to advance a natural product lead through preclinical development. Spliceostatins are polyketide-nonribosomal peptide natural products that bind to the spliceosome, an emerging target in cancer therapy. The wild-type bacterium *Burkholderia* sp. FERM BP-3421 produces a suite of spliceostatin congeners with varying biological activities and physiological stabilities. Hemiketal compounds such as FR901464 were the first to be described. Due to its improved properties, we were particularly interested in a carboxylic acid precursor analog that was first reported from *Burkholderia* sp. MSMB 43 and termed thailanstatin A. Inactivation of the iron/α-ketoglutarate-dependent dioxygenase gene *fr9P* had been shown to block hemiketal biosynthesis. However, a 4-deoxy congener of thailanstatin A was the main product seen in the dioxygenase mutant. We show here that expression of the cytochrome P450 gene *fr9R* is a metabolic bottle neck, as use of an L-arabinose inducible system led to nearly complete conversion of the 4-deoxy analog to the target molecule. By integrating fermentation media development approaches with biosynthetic engineering, we were able to improve production titers of the target compound >40-fold, going from the starting ~60 mg/L to 2.5 g/L, and to achieve what is predominantly a single component production profile. These improvements were instrumental in enabling preclinical development of spliceostatin analogs as chemotherapy.

Keywords: polyketide; biosynthesis; thailanstatin; spliceostatin; splicing inhibitor; antibody drug conjugate.

1. Introduction

Natural products have provided a rich source of new medicines to treat a broad array of diseases including infections, cancer, heart disease, and as immunosuppressants to enable organ transplantion (Li and Vederas, 2009). Yet, natural products have lost favor as a source of leads in the pharmaceutical industry over the past decades, owing to changes in the discovery landscape and the well-recognized difficulties associated with natural products drug discovery. The two major challenges in advancing natural product drug leads are adequate supply and ease of structural modification, which is often needed to improve pharmaceutical properties. Hundreds of grams to kilograms of pure material are necessary to move a hit forward through preclinical development and ultimately clinical trials (Carter, 2011; Li and Vederas, 2009). Supply can be enabled by total synthesis, as elegantly exemplified for perhaps the most complex example, eribulin mesylate – a fully synthetic analog of polyether macrolide halichondrin B that was originally isolated from marine sponges and has been approved for treatment of metastatic breast cancer (Towle et al., 2001). Highly productive microbial sources are an attractive alternative to total synthesis in terms of cost and sustainability. Moreover, recent advancements in genomics and genetic engineering allow the application of "biosynthetic medicinal chemistry" for lead development (Koehn, 2012).

FR901464 (**4**) is a hemiketal natural product that was first isolated from *Burkholderia* sp. FERM BP-3421 (previously identified as *Pseudomonas* sp. No. 2663) (He et al., 2014; Nakajima et al., 1997). A more stable, semi-synthetic analog of FR901464 was later shown to target the spliceosome – an emerging mode of action for anticancer therapy (Bonnal et al., 2012) –, and it was thus termed spliceostatin A (**6**) (Kaida et al., 2007). Compounds containing a terminal carboxylic acid (**1-3**) instead of the hemiketal present in **4** and **5** were later isolated from FERM BP-3421 and from *Burkholderia* sp. MSMB 43 (He et al., 2014; Liu et al., 2013a; Liu et al., 2013b). One of these carboxyl analogs was termed thailanstatin A (**3**) as it was first described from MSMB 43, a *B. thailandensis*-like isolate (Gee et al., 2008; Liu et al., 2013a). For simplicity and in an effort to unify their terminology, we will refer to the class of natural congeners **1**-**5** as spliceostatins (Fig. 1).

Spliceostatin biosynthesis is encoded in a hybrid nonribosomal peptide synthetase (NRPS), polyketide synthase (PKS) gene cluster of the *trans*-acyltransferase (AT) type (Liu et al., 2013a; Zhang et al., 2011). Several total syntheses of FR901464 have been reported (Albert and Koide, 2004; Albert et al., 2007; Albert et al., 2006; Horigome et al., 2001; Motoyoshi et al., 2006; Thompson et al., 2000; Thompson et al., 2001). The shortest described route contains 20 total steps with the longest linear sequence of 10 steps, an overall yield of 5.2% (Ghosh and Chen, 2013; Ghosh et al., 2014), and the largest quantity produced being 20.1 mg (Albert and Koide, 2004; Albert et al., 2007; Albert et al., 2006). We aimed to harness the biosynthetic potential of the producing organism as a viable and sustainable alternative to total synthesis. We were particularly interested in the carboxyl series, as they were shown to inhibit splicing as potently as the hemiketals, while having improved stability (Liu et al., 2013a). When derivatized to increase

cell permeability (e.g. as methyl esters or propyl amides), the carboxyl series exhibits cytotoxicity against cancer cell lines comparable to the hemiketals (He et al., 2014).

Gene inactivation along with biochemical studies led us to propose the biosynthetic scheme depicted in Fig. 1, in which a Flavin-dependent monooxygenase (FMO) domain present in the last module of the PKS Fr9GH catalyzes epoxidation, the cytochrome P450 monoxygenase Fr9R, hydroxylation at C-4, and the iron/α-ketoglutarate-dependent dioxygenase Fr9P, hydroxylation at C-1, which followed by decarboxylation leads to hemiketal **4** (Eustáquio et al., 2014). Epoxidation and hydroxylation at C-4 have been shown to lead to improved potency (Eustáquio et al., 2014; He et al., 2014). Thus, we focused our efforts on carboxyl compound **3**. Our objectives were to attain 1) sustainable compound production in multi-gram scale; and 2) predominantly single-component fermentation to facilitate downstream processing and purification. Our approach was to combine classical fermentation media development to improve overall titers and biosynthetic engineering to block production of hemiketals and increase biosynthesis of **3**. Herein we describe how we attained production of **3** at 2.5 g/L from the starting ~60 mg/L and how a strain was obtained that produces nearly exclusively **3** in detriment of the other spliceostatin congeners.

2. Materials and Methods

2.1. General. Oligonucleotide primers were synthesized by Sigma-Aldrich. Restriction enzymes were from New England Biolabs. Phusion polymerase (Finnzymes) was used in PCR reactions unless otherwise stated. DNA purification was performed using Qiagen kits. DNA sequencing to confirm accuracy of plasmid inserts was routinely performed by Beckman Coulter Genomics. *E. coli* TOP10 cells (Invitrogen) were used for routine cloning. *E. coli* cells for λ-Red-mediated recombination (Datsenko and Wanner, 2000) were obtained from the *E. coli* Genetic Resource Center at Yale University.

2.2. Cultivation conditions and metabolite analysis. FERM BP-3421 was acquired from the international Patent Organism Depository at the National Institute of Advanced Industrial Science and Technology (Tsukuba, Japan), and was routinely cultured in Luria-Bertani (LB) or nutrient broth or agar medium (Becton, Dickinson and Company) at 30 °C, unless otherwise stated. The culture was preserved in 12.5-20% sterile glycerol and stored at -80 °C. For metabolite analyses, seed medium [polypeptone (Bacto Difco) 1% w/v, yeast extract (Bacto Difco) 0.5 % w/v, and sodium chloride (Sigma-Aldrich) 0.5% w/v] was inoculated with a frozen stock or with a "loopful" (10 µL) of agar-grown culture and incubated at 30˚C, 220 rpm overnight. This first seed culture was either used to inoculate a second stage seed at 10% (v/v) which was incubated as above, or it was directly used to inoculate the production medium. Production medium (see below) was inoculated with seed culture at 2.5% (v/v) and incubated at 25˚C, 200 rpm for three days to seven days. Seed cultures were grown either in 14 mL, polypropylene round bottom tubes (BD) containing 5 mL medium or in 250 mL Erlenmeyer flasks containing 50 mL medium. Tetracycline (25 µg/mL) was added where appropriate. Production cultures were grown in 250 mL Erlenmeyer flasks containing 50 ml medium. No antibiotics were added to production cultures. The fermentation was processed with 5% (w/v) Diaion HP-20 resin as previously described (Eustáquio et al., 2014). Alternatively, aliquots of the production culture were diluted with aqueous acetonitrile (1:1) before analysis. After centrifugation and filtering, the sample was analyzed by HPLC and/or LC/MS as previously described (Eustáquio et al., 2014). Production titers were calculated based on a standard curve of pure **3**.

2.3. Fermentation media development. The strain used to optimize the production medium is a natural variant (single colony isolate NS6) of FERM BP-3421. For nitrogen and carbon source evaluation, FERM BP-3421 was streaked onto nutrient agar and incubated at 30 °C for three days. One "loopful" (10 µL) of the three-day old agar culture was inoculated into 50 mL seed medium contained in a 250 mL Erlenmeyer flask and incubated at 30 °C, 200 rpm for 24 h. The production medium optimization was carried out using 50 mL medium in 250 mL Erlenmeyer flasks. The slightly modified, original medium (Nakajima et al., 1996) consisted of soluble starch (BD Difco) 1% w/v, glycerol 1% w/v, dextrose (JT Baker) 0.5% w/v, Hy Soy Soy Peptone (Kerry Biosciences) 1% w/v, corn steep solid (Sigma) 0.25% w/v, $(NH_4)_2SO_4$ (Sigma) 0.2% w/v, $MgSO_4.7H_2O$ (Sigma) 0.006% w/v and $CaCO_3$ (Mississippi lime) 0.2% w/v in distilled water,

and was used as the control. To evaluate the nitrogen source, a basal medium consisted of dextrose (JT Baker) 4% w/v, $(NH_4)_2SO_4$ (Sigma) 0.2% w/v, $MgSO_4 \cdot 7H_2O$ (Sigma) 0.006% w/v and $CaCO_3$ (Mississippi lime) 0.2% w/v in distilled water. Six nitrogen sources, i.e. corn steep solid (Sigma-Aldrich), Hy Soy Soy Peptone (Kerry BioSciences), Brewer's Yeast (Sargent-Welch), Poly Peptone (BD Difco), Pharmamedia (Traders Protein) and wheat gluten (Spectrum), were tested at three concentrations (0.5%, 1%, and 2% w/v). Flasks containing production media were autoclaved at 121 °C for 25 min. Production of spliceostatins was evaluated after 48 and 72 hours as described above. Two replicates were analyzed for each treatment. The nitrogen source and concentration that gave the best titers (soy peptone 2% w/v) was used to evaluate the carbon source. The carbon sources tested included dextrose (Sigma-Aldrich), lactose, sorbitol (Sigma-Aldrich), glycerol (JT Baker), sucrose (JT Baker), soluble starch (BD Difco), honey (Beemaid) and Molasses (Grandma's Original) at a final concentration of 4% (for a complete list see SI Fig. 1).

2.4. Plasmid construction.

pUCP_cat. The 880-bp chloramphenicol resistance gene (*cat*) fragment and the 892-bp *oriT* fragment were amplified by PCR using primer pair P1_cat (GTT GGT TTG CGC ATT CAC AGT TCT CCG CAA GAA TTG ATT GCC TAC CTG TGA CGG AAG ATC AC, homology extension for λ-Red recombination underlined) and P2_cat (ATA GGA ACT TCG GAA TAG GAA CTT C) and pKD3 (Datsenko and Wanner, 2000) as template, and primer pair P3_oriT (CAT TTA AAT GAA GTT CCT ATT CCG AAG TTC CTA TCT AGA GTC GAT CTT CGC CAG CAG, *cat* extension for SOE-PCR underlined) and P4_oriT (AGC TTG AGT ATT CTA TAG TGT CAC CTA AAT AGC TTG GCG GGA TGG CCT TTT TGC GTT TCT AC, homology extension for λ-Red recombination underlined) and pEX100T (Schweizer and Hoang, 1995) as template, respectively. After gel-purification, *cat* and *oriT* were fused by SOE-PCR and the product gel purified. The tetracycline resistance marker (*tet*) in pUCP26 (West et al., 1994) was then replaced by the *cat-oriT* cassette using λ-Red-mediated recombination (Datsenko and Wanner, 2000) to yield pUCP_cat.

pAE-PF20. The 1,742-bp *fr9R* gene was amplified by PCR using primer pair P_P450_f_XbaI (GCTCTAGAGGGAAAACGGTTTTACACCACG, XbaI site underlined) and P_P450_r_HindIII (ATGGTGAAGCTTAAGTCGACAACCGGCATTCC, HindIII site underlined) and Ferm BP-3421 genomic DNA as template. After digestion with XbaI and HindIII, *fr9R* was ligated into the same sites of pUCP_cat to yield pAE-PF20.

pUCP_neo (pAE-PF23). The 1,198-bp *neo* fragment was amplified by PCR using pCR2.1 (Invitrogen) as template and primer pair P1_neo_pCR2.1 (GTT GGT TTG CGC ATT CAC AGT TCT CCG CAA GAA TTG ATT GCA AGG GCT GCT AAA GGA AG, homology extension for λ-Red recombination underlined) and P2_neo_pCR2.1 (ACG GAA ATG TTG AAT ACT CAT ACT C). The 965-bp *oriT* fragment was amplified by PCR using pEX100T as template and primer pair P3_oriT_neo_pCR2.1 (AAA AAG GAA GAG TAT GAG TAT TCA ACA TTT

CCG TCT AGA GTC GAT CTT CGC CAG CAG, *neo* extension for SOE-PCR underlined) and P4_oriT (AGC TTG AGT ATT CTA TAG TGT CAC CTA AAT AGC TTG GCG GGA TGG CCT TTT TGC GTT TCT AC, homology extension for λ-Red recombination underlined). After gel purification of PCR products above, the *neo-oriT* cassette was assembled by SOE-PCR using primer pair P1_neo_pCR2.1 and P4_oriT. The *tet* marker in pUCP26 was replaced with the *neo-oriT* cassette using λ-Red-mediated recombination to yield pUCP_neo.

CTX1_neo (pAE-PF24). A 1,237-bp *neo* fragment was amplified by PCR using pCR2.1 (Invitrogen) as template and primer pair P1_neo_pCR2.1 and P2_neo_tet_CTX1_pCR2.1 (TCT TCC GCT TCC TCG CTC ACT GAC TCG CTG CGC TCG GTC ACG GAA ATG TTG AAT ACT CAT ACT C, homology extension for λ-Red recombination underlined). After treatment of the PCR reaction with DpnI and purification using Qiagen's PCR purification kit, the *neo* cassette was used to replace the *tet* marker in mini-CTX1 (Hoang et al., 2000) using λ-Red-mediated recombination to yield CTX1_neo.

pAE-PF25. The 727-bp S7 promoter fragment was amplified by PCR using FERM BP-3421 genomic DNA as template and primer pair P1_S7p_f (GCT CTA GAC GCA AGC TGT TGA CTC GCT TAG, XbaI site underlined) and P2_S7p_r (GTT TCT TCC TTT GAC TTT TCA GTT G). The *fr9R* P450 gene and its native RBS (1,534 bp fragment) were amplified by PCR using FERM BP-3421 genomic DNA as template and primer pair P3_P450_S7_f (CGC TCC AAC TGA AAA GTC AAA GGA AGA AAC GGG TTG TTG GTT TTT GAA ATT GC, S7 extension for SOE-PCR underlined) and P4_P450_r (ATG GTG AAG CTT AAG TCG ACA ACC GGC ATT CC, HindIII site underlined). The two DNA fragments were assembled by SOE-PCR and ligated into the XbaI and HindIII sites of pUCP_neo to generate pAE-PF25.

pAE-PF26. The 1,215-bp P_{BAD}/araC arabinose inducible system was amplified by PCR using pKD46 (Datsenko and Wanner, 2000) as template and primer pair P1_BADp_f (GCTCTAGACATCGATTTATTATGACAACTTGAC, XbaI site underlined) and P2_BADp_r (CCC AAA AAA ACG GGT ATG G). The fr9R P450 gene and its native RBS (1,534 bp fragment) were amplified by PCR using FERM BP-3421 genomic DNA as template and primer pair P3_P450_BAD_f (CTA CTG TTT CTC CAT ACC CGT TTT TTT GGG GGG TTG TTG GTT TTT GAA ATT GC, extension for SOE-PCR underlined) and P4_P450_r (see above). The two DNA fragments were assembled by SOE-PCR and ligated into the XbaI and HindIII sites of pUCP_neo to generate pAE-PF26.

pAE-PF27. The 1,742-bp *fr9R* gene fragment obtained as described for pAE-PF20 was ligated into the XbaI and HindIII sites of pUCP_neo to generate pAE-PF27.

pAE-PF28. The S7-P450 fragment obtained by SOE-PCR as described above for pAE-PF25 was ligated into the SpeI-HindIII sites of CTX1_neo to give pAE-PF28.

pAE-PF29. The P_{BAD}/araC-P450 fragment obtained by SOE-PCR as described above for pAE-PF26 was ligated into the SpeI-HindIII sites of CTX1_neo to give pAE-PF29.

pAE-PF30. The 1,742-bp *fr9R* gene fragment obtained as described for pAE-PF20 was ligated into the SpeI and HindIII sites of CTX1_neo to generate pAE-PF30.

2.5. Generation of FERM BP-3421 mutants. Plasmid DNA was transferred into FERM BP-3421 by conjugation from *E. coli* S17 as previously described (Eustáquio et al., 2014). Chloramphenicol (100-200 µg/ml for the dioxygenase mutant of Ferm BP-3421, and 25 µg/ml for *E. coli*) and kanamycin (500 µg/ml for the dioxygenase mutant of Ferm BP-3421, and 50 µg/ml for *E. coli*) were used for selection. Gentamycin (10 µg/ml) was used to remove *E. coli* after conjugation. Mutants were confirmed by PCR.

2.6. Bioreactor fermentation of the *fr9P*$^{-}$ mutant containing pAE-PF29 at low dissolved oxygen. The *fr9P*$^{-}$ mutant containing pAE-PF29 was cultured in seed medium as described above. 250 ml of a second stage seed culture was used to inoculate 10L of production medium (4% glycerol, 1.5% L-arabinose, 2% HySoy soy peptone, 0.2% ammonium sulfate, 0.01% magnesium sulfate heptahydrate, 0.2% calcium carbonate) contained in a 14-L (10L working volume) Bioreactor (BioFlo310® , New Brunswick Systems, with Biocommand Batch Control/v.5.1.2600 software). The fermentation was carried out at 25°C for 116 hours. Initial agitation was set at 400 rpm; pH was controlled at 7.4; Dissolved oxygen (DO) was controlled at 6% with increased agitation, up to 900 rpm. SE-15 (10% silicone emulsion, Sigma-Aldrich) was used to control foaming. Samples were taken daily and the fermentation supernatant was analyzed by HPLC. Titers are shown in SI Table 1. One kilogram of wet DIAION HP-20 resin was added to the whole broth and the mixture was shaken for three hours. The HP-20 was collected by filtration through a 50µm-150µm stainless steel wedge wire mesh. The compound-bound HP-20 resin was extracted three times, each with ~3L ethyl acetate with shaking for 1 h. The ratio of recovered **3** and **2** differed from the raw tank titers (supernatant analysis) due to different recovery efficiencies for **3** and **2** indicating that more solvent should be used for full recovery of **3** (SI Table 1).

2.7. Bioreactor fermentation of the *fr9P*$^{-}$ mutant containing pAE-PF29 at elevated dissolved oxygen. Two Bioreactors containing 10 L of production medium each were inoculated as described above. The fermentation was carried out at 25°C for 86 hours. Initial agitation was set at 450 rpm in both vessels; pH was initially adjusted to 7.5 but not controlled further. DO was maintained at 40% in bioreactor 1 and 60% in bioreactor 2 by means of increased agitation (450-1,200 rpm). The initial airflow was 5 SLPM (ramped to 10 SLPM for DO control) in both vessels. Foaming was controlled by addition of SE-15 antifoam. Additionally, three 2.8L Fernbach control flasks containing 550 ml production medium were each inoculated with 13.75 ml of second stage seed. Samples were taken daily and analyzed by HPLC. Titers are shown in SI Table 2. A total of 16L whole broth from both bioreactors (~2 L were removed during the run to control foaming) was pooled at 86 hours, and 1.5 kg of wet DIAION HP-20 resin was added, and the mixture was shaken for three hours. The HP-20 and cell mass was processed as described above and extracted four times with 2L of ethyl acetate. The combined ethyl acetate

extract was dried under reduced pressure to give 30 grams of **3** as a light-yellow powder at ~55% purity by UV (230 nm).

3. Results and Discussion

3.1. Fermentation media development

The published spliceostatin production medium (Nakajima et al., 1996) contains soluble starch (1%), glycerol (1%) and glucose (0.5%) as carbon sources; and defatted soy meal (1%), corn steep liquor (0.5%) and ammonium sulfate (0.2%) as nitrogen sources. All concentrations are w/v unless otherwise stated. In order to simplify and optimize the production medium we took a "one variable at a time" approach (Masurekar, 2008) in which six commonly used, complex nitrogen sources were first investigated at three concentrations, including the two present in the original medium (Fig. 2a). All mineral ingredients present in the original medium (ammonium sulfate, magnesium sulfate and calcium carbonate) were included in the basal media, along with 4% glucose to support growth as previously reported for *Pseudomonas fluorescens* (Ikeda et al., 1983). Of the six nitrogen sources tested, 2% soy peptone over a three-day fermentation gave the best titers at 0.72 g/L total spliceostatins (sum of **1**-**5**), compared to 0.37 g/L for the original medium. Note that titers rise with increasing concentrations of soy peptone (from 0.5% to 2%); whereas, there was an adverse effect on titers at the 2% polypetone concentration. It remains to be shown if higher soy peptone concentrations may lead to further titer increase. Cultures grown in the presence of corn steep solid (replacement for the liquor in the original medium) showed no detectable spliceostatin production, therefore it could be eliminated from the formula. Wheat gluten yielded ≤25 mg/L total titers. Brewer's yeast and Pharmamedia® led to no detectable spliceostatins and are, therefore, not adequate nitrogen sources for spliceostatin production (Fig. 2a).

Various carbon sources, including those present in the original medium, were investigated next. 2% Soy peptone was used as the nitrogen source in these studies and all mineral ingredients were kept constant as in the original medium. Carbon sources tested included monosaccharides, disaccharides, polysaccharides, sugar alcohols, and crude sources such as molasses (SI Fig. 1). Soluble starch, which is one of the originally published ingredients (Nakajima et al., 1996), did not support spliceostatin production when used as the sole carbon source; in fact, the strain has been shown to not hydrolyze starch (Nakajima et al., 1996). The three carbon sources (4% concentration (Ikeda et al., 1983)) that yielded the best titers at the three-day time point analyzed, i.e. glycerol, sorbitol and glucose, were retested (Fig. 2b). It should be noted that when increasing the fermentation from three to four days, titers continued to increase, particularly for glycerol. Glycerol was established as the preferred carbon source, leading to 1.1 g/L total spliceostatins after four days fermentation. The simplified and optimized medium was named 2S4G (2% soy peptone, 4% glycerol, 0.2% ammonium sulfate, 0.006% magnesium sulfate

heptahydrate, and 0.2% calcium carbonate). Because titers continued to increase from day three to four, longer fermentation times were investigated in later experiments.

3.2. Comparison of metabolite titers produced by the wild-type and the *fr9P*$^{-}$ mutant strains in published and optimized media

We have previously shown that the iron/α-ketoglutarate-dependent dioxygenase Fr9P catalyzes hydroxylation at C-1, which followed by decarboxylation leads to hemiketal **4** (Fig. 1) (Eustáquio et al., 2014). Accordingly, the *fr9P*$^{-}$ mutant produces only carboxyl-bearing members of the suite, i.e. compounds **1**, **2** and **3**. Titers for the wild-type and mutant strains in the published and optimized 2S4G production media over time are shown in Fig. 3. The 2S4G production medium led to a 5-fold increase in total titers for the wild-type (at day 3) and to a 9-fold increase for the mutant (at day 5), compared to the original, published medium. Note that total titers for the wild-type decreased from day 3 to 5, while increasing for the mutant in the same time period (day 4 aliquots were not analyzed). The maximum total titer obtained with the wild-type strain in the optimized medium in this experiment was 1.05 g/L at day 3, whereas the mutant strain produced 4.35 g/L total at day 5. The higher titer observed with the mutant strain may be due to increased stability of carboxyl spliceostatins (half-life at pH 7.4 of >8 days) over the hemiketals (half-life at pH 7.4 of <17 h).

The 2S4G medium is richer than the original medium (4% carbon source in 2S4G *vs*. 1.5% effective (since starch is not utilized) carbon source in the published medium and 2% *vs*. 1.5% nitrogen source, respectively), resulting in a prolonged growth period and in higher cell mass. When normalized by cell mass (SI Fig. 2), the 2S4G medium still affords an increase in total titers in comparison to the original medium, i.e. 2.8-fold for the wild-type and 4.7-fold for the mutant, indicating that factors other than cell mass alone are contributing to titer increase. Media composition, e.g. the type of carbon and nitrogen source used, also affects titers, as it would be expected and as shown above (Fig. 2). The yield of total spliceostatins for the *fr9P*$^{-}$ mutant was 109 mg/g glycerol in the 2S4G medium.

The *fr9P*$^{-}$ mutant was generated by replacing *fr9P* with a tetracycline-resistance marker (*tet*). We observed that adding tetracycline (25 mg/L) to seed cultures leads to increase in total titers in both the 2S4G (6.36 g/L *vs*. 4.35 g/L at day 5) and in the original medium (1.4 g/L *vs*. 0.6 g/L at day 3) compared to using seed cultures without tetracycline to inoculate the production media. No tetracycline was added to production cultures besides what is carried over with the seed (Fig. 4). Sub-inhibitory concentrations of antibiotics have been shown to activate natural product biosynthesis, as recently exemplified with *Burkholderia thailandensis* (Seyedsayamdost, 2014).

Titers of **3** in the 2S4G optimized medium were improved 1.8-fold in the mutant when directly compared to the wild-type (347 mg/L *vs*. 195 mg/L, respectively, at day 5) and 4-fold when using mutant seed cultures containing tetracycline (794 mg/L *vs*. 195 mg/L, respectively, at day

5). However, the main product produced by the *fr9P*$^{-}$ mutant was **2** (4 g/L and 5.6 g/L when using seed cultures without or with tetracycline, respectively). Inactivation of cytochrome P450 gene *fr9R* leads to a mutant that produces only 4-deoxy analogs (Eustáquio et al., 2014). Therefore, Fr9R is hypothesized to function as a 4-hydroxylase. Thus, we focused next on the step putatively catalyzed by Fr9R to attempt improving conversion of **2** to **3**.

3.3. Identifying the limiting factor in the cytochrome P450 Fr9R reaction

Cytochrome P450 (CYP) enzymes form a large family of hemoproteins that catalyze diverse oxidative reactions, including hydroxylation of saturated C−H bonds. Iron(III) protoporphyrin-IX is covalently linked to a cysteine side chain in CYPs as a prosthetic group. All CYPs are part of a multi-enzymatic system. Most bacterial CYP complexes are soluble and consist of three separate proteins, i.e. CYP, a NAD(P)H-dependent, flavin-containing oxidoreductase (ferredoxin reductase), and an iron-sulfur protein (ferredoxin), which transfers electrons from the ferredoxin reductase to CYP. Molecular oxygen is used as the oxidant, in which one of its oxygen atoms is inserted into the substrate, and the second reduced to a water molecule, in a process utilizing electrons from NAD(P)H via the redox partner proteins (Meunier et al., 2004).

We decided to test first if either iron or heme availability are insufficient to support the Fr9R-catalyzed reaction under the culture conditions used for spliceostatin production (2S4G medium). Supplementation of $FeCl_3$ (0.2 mM) and/or δ-aminolevulinic acid (0.5 mM) as a heme precursor (Harnastai et al., 2006) had no significant effect on the ratio of **3** to **2**, indicating that neither Fe(III) nor heme availability are limiting factors under the culture conditions analyzed. We next explored the possibility that *fr9R* expression may be lower than necessary for complete conversion of **2** to **3**. To test this hypothesis, we cloned *fr9R* and its own putative promoter onto the self-replicating plasmid pUCP_cat, a derivative of pUCP26 (West et al., 1994) in which *tet* was replaced by a *cat*/*oriT* (chloramphenicol-resistance gene/origin of transfer) cassette to allow selection in the dioxygenase mutant and DNA transfer by conjugation from *E. coli*. Mutants containing the plasmid so generated, pAE-PF20, showed a 6-fold increase in **3** to **2** ratios, going from 0.13 to 0.8 (Fig. 5a). These results indicated that the expression of the *fr9R* gene is limiting production of **3**.

3.4. Expression of CYP gene *fr9R* under an L-arabinose-inducible promoter leads to nearly one-component fermentation

Encouraged by the promising results with overexpression of CYP gene *fr9R*, we next focused on identifying an expression system that would allow nearly complete conversion of **2** to **3**. Two vector types were chosen (self-replicative and integrative), along with three promoters (constitutive, inducible, and *fr9R*'s native promoter as control). From our experiments with

pUCP_cat, we determined that chloramphenicol resistance is not an ideal selection marker for the dioxygenase mutant of *Burkholderia* sp. FERM BP-3421 due to background growth even at high concentrations, yielding false positives and a low number of exconjugants, i.e. conjugation had to be attempted several times until mutants were obtained. Thus, we decided to use *neo*, a neomycin/kanamycin resistance gene, as a selection marker instead. Derivatives of pUCP26 (replicative) and mini-CTX1 (integrative) vectors were generated in which *tet* was replaced by *neo-oriT* and *neo*, yielding pUCP_neo and CTX1_neo, respectively. For a constitutive promoter, we chose to use the promoter from ribosomal protein S7 from FERM BP-3421. For an inducible promoter, we chose the P_{BAD}/araC system from *E. coli*. FERM BP-3421 does not utilize L-arabinose as carbon source (Nakajima et al., 1996), which should then serve only as inducer of the P_{BAD} promoter. The S7 and P_{BAD} promoters have been previously shown to function well in *Burkholderia cepacia* (Lefebre and Valvano, 2002). *fr9R*'s native promoter was used as control. Each plasmid was transferred into the dioxygenase mutant by conjugation from *E. coli*. The results are summarized in Fig. 5.

The promoter that gave the most desirable **3**/**2** ratios was the P_{BAD}/araC system from *E. coli*, i.e. average of 22 when using a self-replicative vector (pAE-PF26) and 16 for the integrative vector (pAE-PF29) at day 5 in 2S4G medium (Fig. 5a). Although overexpression of CYP gene *fr9R* leads to increased **3**/**2** ratios in all cases except with pAE-PF30 (own promoter, integrative vector), it comes at the expense of ≥2-fold reduced total titer (Fig. 5b), the exceptions being integrative vectors pAE-PF30 and pAE-PF28 (S7 promoter). Self-replicative plasmids appear to be a particular burden, because all mutants containing self-replicative plasmids showed a reduction in total titer, even the ones that led to only a modest improvement in **3**/**2** ratios, whereas for the integrative plasmids only the one containing the L-arabinose- inducible promoter showed a significant drop in total titer. We chose to continue with pAE-PF29 as it yielded the best **3**/**2** ratios and total titer combination. An additional advantage of pAE-PF29 is that a mutant containing a chromosomally integrated copy of the CYP gene *fr9R* should be more stable than one containing a self-replicative plasmid.

Fig. 6 shows that an increase in L-arabinose concentrations leads to a desired increase in **3**/**2** ratios, while resulting in a reduction in total titer. Two hypotheses may explain this observation. First, high expression of the CYP gene *fr9R* is metabolically taxing, leading to a reduction in production titer. Second, addition of L-arabinose to the production medium may have an adverse effect on production titer that is independent of *fr9R* expression. To test the latter, we carried out a control fermentation using the parent strain (the *fr9P*$^{-}$ mutant without a CYP plasmid) in which 100 mM L-arabinose was added to the medium. L-arabinose addition led to a 1.6-fold reduction in total titer compared to having no L-arabinose in the medium (3.4 ± 0.1 *vs.* 5.5 ± 0.1 g/L). Thus, it appears that L-arabinose itself accounts for at least some of the observed reduction in total titer, independently of increased *fr9R* expression. In fact, L-arabinose at >0.1 g/L has been shown to inhibit growth of an engineered *E. coli* strain which is unable to catabolize L-arabinose and to decrease titers of the bis-indole natural product deoxyviolacein (Rodrigues et al., 2014).

We observed a 1.4-fold reduction in cell mass at high inducer concentrations (100 mM, =15 g/L). When normalized by cell mass, there is still a 1.7-fold reduction in total titer in the presence of inducer, i.e. the *fr9P*$^{-}$ mutant containing pAE-PF29 produces 98 mg total spliceostatins per g wet cell mass in the absence of inducer and 57 mg total spliceostatins per g wet cell mass in the presence of 100 mM L-arabinose. Thus, a reduction in cell mass contributes to the adverse effect of L-arabinose induction, but does not seem to explain it completely. In fact, increased *fr9R* expression may contribute to a reduction in overall spliceostatin yield as well, because a ≥2-fold drop in total titer is observed with most mutants overexpressing CYPs as discussed above (Fig. 5b). Further studies are necessary to understand the mechanism of yield reduction in detail.

To investigate whether the issue of overall titer reduction caused by L-arabinose supplementation can be circumvented, we tested adding the inducer at different time points during the fermentation. However, addition of L-arabinose at days one through five followed by harvest after 6-7 days did not lead to any improvements (Fig. 7, results for day 6 shown). Induction of the CYP gene *fr9R* with L-arabinose at the time of inoculation gave the best **3** titers and **3**/**2** ratios. Induction at day 2 or later led to **3**/**2** ratio <1.

With the *fr9P*$^{-}$ mutant containing pAE-PF29, we reached both our goals of sustainable compound production in gram scale and nearly one component fermentation. The yield of **3** by the *fr9P*$^{-}$/pAE-PF29 mutant was 62 mg per g glycerol in the 2S4G medium with 100 mM L-arabinose. It remains to be shown if further media optimization in which interactions between media components would be evaluated (including L-arabinose), along with testing different promoters for *fr9R* expression may lead to further yield improvements.

3.5. Bioreactor fermentation

Once we had achieved high titer and nearly a single component profile in flasks, we sought to develop the bioprocess in 10L bioreactors. The *fr9P*$^{-}$ mutant containing pAE-PF29 was fermented in 10L stirred bioreactors using the flask-optimized 2S4G medium containing 100 mM L-arabinose. Production was robust and the ratio of the metabolites **3** and **2** was dependent on dissolved oxygen. Tank fermentation at 6% dissolved oxygen gave a broth titer of 2.5 g/L of **3** and 0.93 g/L of **2** at 116 hours, with a **3**/**2** ratio of 2.7:1. Raising the dissolved oxygen to 60% gave **3** at 2.4 g/L and **2** at 0.15 g/L, and a **3**/**2** ratio of 16:1 at 86 hours. Overall, a 16L portion of the bioreactor fermentation at high dissolved oxygen furnished 30 g of crude **3** at ~55% purity after solid phase extraction. This crude **3** fermentation product was routinely used as substrate for synthetic chemistry without further purification.

4. Conclusions

In conclusion, by integrating fermentation media development approaches with biosynthetic engineering, we were able to improve production titers of the target compound >40-fold. Fig. 8 summarizes titer improvement of **3** in each step of the optimization process in flask fermentation (see also SI Figure 3 for a summarized comparison to total titers). From the starting ~60 mg/L (step 1), investigation of different carbon and nitrogen sources allowed media simplification and 3.2-fold titer improvement with the wild-type strain (step 2, 195 mg/L). Inactivation of the dioxygenase gene *fr9P* blocked biosynthesis of hemiketals, yielding a mutant that produces only carboxylic acid analogs (step 3, 347 mg/L **3** in optimized medium). Addition of tetracycline to seed cultures of the *fr9P*$^{-}$ mutant strain increased titers 2.3-fold (step 4, 794 mg/L). However, congener **2** was the main component in the fermentation. Subsequently, expression of the CYP gene *fr9R* under the *E. coli* L-arabinose inducible promoter led to nearly one-component fermentation, with the desired analog **3** being produced at 2.5 g/L (step 5). The fact that overexpression of CYP gene *fr9R* improves conversion of **2** to **3**, serves as further evidence that Fr9R functions as a 4-hydroxylase as suggested by gene inactivation studies (Eustáquio et al., 2014). In addition, the bioprocess can be scaled up to bioreactors in which titers and **3**/**2** ratios are comparable to flask fermentation. The crude extract is ~55% pure and can be used directly for structure modification by semi-synthesis. If >90% purity is desired, a simple flash chromatography step can be included in the isolation process, without the need for HPLC purification. Finally, production of **3** at high titers was instrumental in moving it forward as a payload for antibody-drug conjugates (Dirico, 2014).

Author Information

Corresponding author

*Email: ase@uic.edu

Author Contributions

ASE designed and performed biosynthetic engineering studies; LPC designed and performed fermentation media development studies; GLS performed bioreactor studies. All authors analyzed and discussed data. ASE wrote the paper. All authors commented on the manuscript.

Notes

The authors are Pfizer employees and stockholders or were at the time that this study was conducted. This study was sponsored by Pfizer Inc.

Acknowledgments

We thank H. P. Schweizer (Colorado State University) for vectors pUCP26, mini-CTX1 and pEX100T, Andrew Tomaras (Biotherapeutics, Pfizer) for supportive discussions on *Burkholderia* genetics, and Haiyin He, Anokha Ratnayake, Jeffrey Janso, Chakrapani Subramanyam, Andreas Maderna, Russell Dushin, Edmund Graziani, and many others for helpful discussions during the course of these studies.

Figure Legends

Figure 1. **Structures of spliceostatin analogs and biosynthetic hypothesis**. FR901464 (**4**) and FR901465 (**5**) are natural products with potent anticancer activity but that is unstable. Spliceostatin A (**6**) is a semi-synthetic analog of **4** with improved stability (Kaida et al., 2007). The carboxyl series has been shown to inhibit the spliceosome as potently as the hemiketals (Liu et al., 2013a) and to exhibit comparable cytotoxicity when derivatized to increase cell permeability (He et al., 2014). We were particularly interested in **3** as epoxidation and hydroxylation at C-4 improves potency and due to its increased stability compared to **4, 5** and **6**. In addition, the carboxyl group offers a convenient handle for downstream synthetic efforts (He et al., 2014). FMO, flavin-dependent monooxygenase domain present in PKS Fr9GH; Fr9R, cytochrome P450 monooxygenase; Fr9P, iron/α-ketoglutarate-dependent dioxygenase (Eustáquio et al., 2014).

Figure 2. **Fermentation media development**. (**a**) Effect of the nitrogen source on total spliceostatin production (sum of **1** to **5**) using 4% glucose as the carbon source. Results shown are an average of N=2 ± standard deviation. (**b**) Effect of selected carbon sources (4%) on total spliceostatin production using 2% soy peptone as the nitrogen source. Original, published medium was used as the control and contained soluble starch (1%), glycerol (1%) and glucose (0.5%) as carbon sources, and defatted soy meal (1%) and corn steep liquor (0.5%) as nitrogen sources. Concentrations are w/v. Results shown are an average of N=3 ± standard deviation. Because titers doubled from day two to day three in panel a (soy peptone), the experiment in panel b was carried out for a longer time period of four days total.

Figure 3. **Comparison of metabolite titers produced by *Burkholderia* sp. FERM BP-3421 wild-type and *fr9P*$^{-}$ dioxygenase mutant.** (**a**) Time-course of total spliceostatins (sum of **1** to **5**) produced by the wild-type (WT) strain in original (orange) and optimized, 2S4G medium (red), and time-course of total spliceostatins (sum of **1** to **3**) produced by the *fr9P*$^{-}$ mutant (mt) strain in original (blue) and optimized, 2S4G medium (purple). Average titers of N=3 ± standard deviation are shown. (**b**) Representative HPLC chromatograms of wild-type and *fr9P*$^{-}$ mutant strains in 2S4G medium at day 3 and 5, respectively. Culture supernatants were diluted as indicated before HPLC analysis with detection at 230 nm.

Figure 4. Influence of tetracycline in seed cultures of the *fr9P*$^{-}$ mutant on spliceostatin total titers. Time-course of total spliceostatins (sum of **1** to **3**) produced by the *fr9P*$^{-}$ mutant strain in original medium using seed cultures with (light blue) and without tetracycline (tet, dark blue) and in 2S4G medium using seed cultures with (green) and without tetracycline (purple). Average titers of N=3 ± standard deviation.

Figure 5. **Expression of CYP gene *fr9R* under different promoters and using replicative or integrative plasmids**. (**a**) Effect on **3**/**2** ratios depending on promoter used (own, *fr9R* upstream region containing a promoter predicted with BPROM (Solovyev, 2011); S7, constitutive

promoter of S7 ribosomal protein from FERM BP-3421; P_{BAD}, P_{BAD}/araC L-arabinose inducible system from *E. coli* with 100 mM L-arabinose), and on vector type (self-replicative, based on pUCP26; and integrative, based on mini-CTX1). The *y* axis is shown in log scale. Cultivation was carried out in 2S4G medium for 5 days using seed cultures containing tetracycline (25 mg/L). Plasmid description: pAE-PF20, *fr9R* and its own putative promoter ligated into vector pUCP_cat; pAE-PF25, 26 and 27, *fr9R* and the promoter indicated ligated into vector pUCP_neo; pAE-PF28, 29 and 30, *fr9R* and the promoter indicated ligated into vector CTX1_neo. (**b**) Effect of CYP gene *fr9R* expression on spliceostatin total titers. Data compiled from three separate experiments and normalized to the total titers obtained with the *fr9P*$^{-}$ mutant control (no plasmid). N=3 ± standard deviation. The color scheme and cultivation conditions are the same as in panel **a**.

Figure 6. Influence of L-arabinose induction of CYP gene *fr9R* on spliceostatin profile and titers. *fr9P*$^{-}$ mutant containing pAE-PF29 cultivated under increasing concentrations of L-arabinose for five days in 2S4G medium. L-arabinose was added at time of inoculation. (**a**) HPLC traces of diluted culture supernatants with detection at 230 nm. (**b**) Total spliceostatin titer (sum of **1** to **3**, red) and **3** titers (blue). Average of N=3 ± standard deviation are shown.

Figure 7. **Effect of time of induction of CYP gene *fr9R* with L-arabinose.** *fr9P*$^{-}$ mutant containing pAE-PF29 to which L-arabinose was added at different time points. Cultivation was carried out for six days in 2S4G medium. Total spliceostatin titer (sum of **1** to **3**, red) and **3** titers (blue). Average of N=2 ± standard deviation. Total titer for the control culture without L-arabinose at day 6 was 5,539 ± 181 mg/l, and titer of **3** was 530 ± 17 mg/l.

Figure 8. Titer improvement. Titer of **3** in each step of the optimization process: (1) starting point, i.e. wild-type strain in published medium. (2) wild-type strain in 2S4G medium. (3) *fr9P*$^{-}$ mutant in 2S4G medium. (4) *fr9P*$^{-}$ mutant (seed culture with tetracycline) in 2S4G medium. (5) *fr9P*$^{-}$/pAE-PF29 mutant (seed culture with tetracycline) in 2S4G medium with 100 mM L-arabinose. Average of N≥2 ± standard deviation.

References

Albert, B. J., Koide, K., 2004. Synthesis of a C4-epi-C1-C6 fragment of FR901464 using a novel bromolactolization. Org. Lett. 6**,** 3655-8.

Albert, B. J., Sivaramakrishnan, A., Naka, T., Czaicki, N. L., Koide, K., 2007. Total syntheses, fragmentation studies, and antitumor/antiproliferative activities of FR901464 and its low picomolar analogue. J. Am. Chem. Soc. 129**,** 2648-59.

Albert, B. J., Sivaramakrishnan, A., Naka, T., Koide, K., 2006. Total synthesis of FR901464, an antitumor agent that regulates the transcription of oncogenes and tumor suppressor genes. J. Am. Chem. Soc. 128**,** 2792-3.

Bonnal, S., Vigevani, L., Valcarcel, J., 2012. The spliceosome as a target of novel antitumour drugs. Nat. Rev. Drug Disc. 11**,** 847-59.

Carter, G. T., 2011. Natural products and Pharma 2011: Strategic changes spur new opportunities. Nat. Prod. Rep. 28**,** 1783-1789.

Datsenko, K. A., Wanner, B. L., 2000. One-step inactivation of chromosomal genes in Escherichia coli K-12 using PCR products. Proc. Natl. Acad. Sci. U. S. A. 97**,** 6640-5.

Dirico, K. J., Eustáquio, A.S., Green, M. E., He, H., He, M., Koehn, F.E., O'Donnell, C.J., Puthenveetil, S., Ratnayake, A.S., Subramanyam, C., 2014. Preparation of spliceostatin analog antibody conjugates for cancer treatment. WO 2014068443.

Eustáquio, A. S., Janso, J. E., Ratnayake, A. S., O'Donnell, C. J., Koehn, F. K., 2014. Spliceostatin hemiketal biosynthesis in Burkholderia spp. is catalyzed by an iron/α-ketoglutarate-dependent dioxygenase. Proc. Natl. Acad. Sci. U. S. A. 111, E3376-E3385.

Gee, J. E., Glass, M. B., Novak, R. T., Gal, D., Mayo, M. J., Steigerwalt, A. G., Wilkins, P. P., Currie, B. J., 2008. Recovery of a Burkholderia thailandensis-like isolate from an Australian water source. BMC Microbiol. 8**,** 54.

Ghosh, A. K., Chen, Z. H., 2013. Enantioselective syntheses of FR901464 and spliceostatin A: potent inhibitors of spliceosome. Org. Lett. 15**,** 5088-5091.

Ghosh, A. K., Chen, Z. H., Effenberger, K. A., Jurica, M. S., 2014. Enantioselective total syntheses of FR901464 and spliceostatin A and evaluation of splicing activity of key derivatives. J. Org. Chem. 79**,** 5697-709.

Harnastai, I. N., Gilep, A. A., Usanov, S. A., 2006. The development of an efficient system for heterologous expression of cytochrome P450s in Escherichia coli using hemA gene co-expression. Protein Expr. Purif. 46**,** 47-55.

He, H. Ratnayake, A. S., Janso, J. E, He, M., Yang, H. Y., Loganzo F., Shor, B., O'Donnell, C. J., Koehn, F. K., 2014. Cytotoxic spliceostatins from Burkholderia sp. and their semisynthetic analogues. J. Nat. Prod. 77, 1864-1870.

Hoang, T. T., Kutchma, A. J., Becher, A., Schweizer, H. P., 2000. Integration-proficient plasmids for Pseudomonas aeruginosa: site-specific integration and use for engineering of reporter and expression strains. Plasmid 43**,** 59-72.

Horigome, M., Motoyoshi, H., Watanabe, H., Kitahara, T., 2001. A synthesis of FR901464. Tetrahedron Lett. 42**,** 8207-8210.

Ikeda, Y., Matsuki, H., Ogawa, T., Munakata, T., 1983. Safracins, new antitumor antibiotics. II. Physicochemical properties and chemical structures. J. Antibiot. 36**,** 1284-9.

Kaida, D., Motoyoshi, H., Tashiro, E., Nojima, T., Hagiwara, M., Ishigami, K., Watanabe, H., Kitahara, T., Yoshida, T., Nakajima, H., Tani, T., Horinouchi, S., Yoshida, M., 2007. Spliceostatin A targets SF3b and inhibits both splicing and nuclear retention of pre-mRNA. Nat. Chem. Biol. 3**,** 576-83.

Koehn, F. E., 2012. Biosynthetic medicinal chemistry of natural product drugs. Med. Chem. Comm. 3**,** 854-865.

Lefebre, M. D., Valvano, M. A., 2002. Construction and evaluation of plasmid vectors optimized for constitutive and regulated gene expression in Burkholderia cepacia complex isolates. Appl. Environ. Microbiol. 68**,** 5956-64.

Li, J. W., Vederas, J. C., 2009. Drug discovery and natural products: end of an era or an endless frontier? Science 325**,** 161-5.

Liu, X., Biswas, S., Berg, M. G., Antapli, C. M., Xie, F., Wang, Q., Tang, M. C., Tang, G. L., Zhang, L., Dreyfuss, G., Cheng, Y. Q., 2013a. Genomics-guided discovery of thailanstatins A, B, and C As pre-mRNA splicing inhibitors and antiproliferative agents from Burkholderia thailandensis MSMB43. J. Nat. Prod. 76**,** 685-93.

Liu, X., Biswas, S., Tang, G. L., Cheng, Y. Q., 2013b. Isolation and characterization of spliceostatin B, a new analogue of FR901464, from Pseudomonas sp. No. 2663. J. Antibiot. 66**,** 555-8.

Masurekar, P. S., 2008. Nutritional and engineering aspects of microbial process development. Prog. Drug Res. 65**,** 291, 293-328.

Meunier, B., de Visser, S. P., Shaik, S., 2004. Mechanism of oxidation reactions catalyzed by cytochrome P450 enzymes. Chem. Rev. 104**,** 3947-80.

Motoyoshi, H., Horigome, M., Watanabe, H., Kitahara, T., 2006. Total synthesis of FR901464: second generation. Tetrahedron 62**,** 1378-1389.

Nakajima, H., Sato, B., Fujita, T., Takase, S., Terano, H., Okuhara, M., 1996. New antitumor substances, FR901463, FR901464 and FR901465. I. Taxonomy, fermentation, isolation, physico-chemical properties and biological activities. J. Antibiot. 49**,** 1196-203.

Nakajima, H., Takase, S., Terano, H., Tanaka, H., 1997. New antitumor substances, FR901463, FR901464 and FR901465. III. Structures of FR901463, FR901464 and FR901465. J. Antibiot. 50**,** 96-9.

Rodrigues, A. L., Becker, J., de Souza Lima, A. O., Porto, L. M., Wittmann, C., 2014. Systems metabolic engineering of Escherichia coli for gram scale production of the antitumor drug deoxyviolacein from glycerol. Biotechnol. Bioeng. 111, 2280-2289.

Schweizer, H. P., Hoang, T. T., 1995. An improved system for gene replacement and xylE fusion analysis in Pseudomonas aeruginosa. Gene 158**,** 15-22.

Seyedsayamdost, M. R., 2014. High-throughput platform for the discovery of elicitors of silent bacterial gene clusters. Proc Natl Acad Sci U S A. 111**,** 7266-71.

Solovyev, V. S., A., 2011. Automatic Annotation of Microbial Genomes and Metagenomic Sequences. In Metagenomics and its Applications in Agriculture, Biomedicine and Environmental Studies (Li, R. W., Ed.), pp 61-78, Nova Science Publishers.

Thompson, C. F., Jamison, T. F., Jacobsen, E. N., 2000. Total synthesis of FR901464. Convergent assembly of chiral components prepared by asymmetric catalysis. J. Am. Chem. Soc. 122**,** 10482-10483.

Thompson, C. F., Jamison, T. F., Jacobsen, E. N., 2001. FR901464: total synthesis, proof of structure, and evaluation of synthetic analogues. J. Am. Chem. Soc. 123**,** 9974-83.

Towle, M. J., Salvato, K. A., Budrow, J., Wels, B. F., Kuznetsov, G., Aalfs, K. K., Welsh, S., Zheng, W., Seletsky, B. M., Palme, M. H., Habgood, G. J., Singer, L. A., Dipietro, L. V., Wang, Y., Chen, J. J., Quincy, D. A., Davis, A., Yoshimatsu, K., Kishi, Y., Yu, M. J., Littlefield, B. A., 2001. In vitro and in vivo anticancer activities of synthetic macrocyclic ketone analogues of halichondrin B. Cancer Res. 61**,** 1013-21.

West, S. E., Schweizer, H. P., Dall, C., Sample, A. K., Runyen-Janecky, L. J., 1994. Construction of improved Escherichia-Pseudomonas shuttle vectors derived from pUC18/19 and sequence of the region required for their replication in Pseudomonas aeruginosa. Gene 148**,** 81-6.

Zhang, F., He, H. Y., Tang, M. C., Tang, Y. M., Zhou, Q., Tang, G. L., 2011. Cloning and elucidation of the FR901464 gene cluster revealing a complex acyltransferase-less polyketide synthase using glycerate as starter units. J. Am. Chem. Soc. 133**,** 2452-62.

Figure 1

Click here to download high resolution image

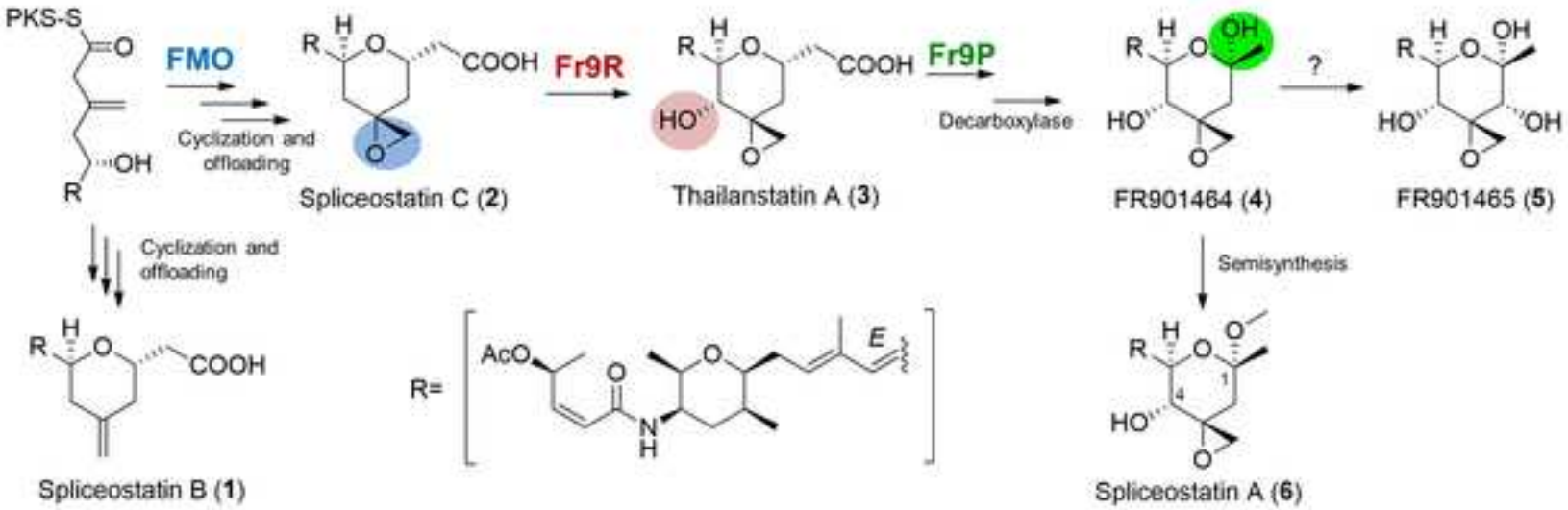

Figure 2

Click here to download high resolution image

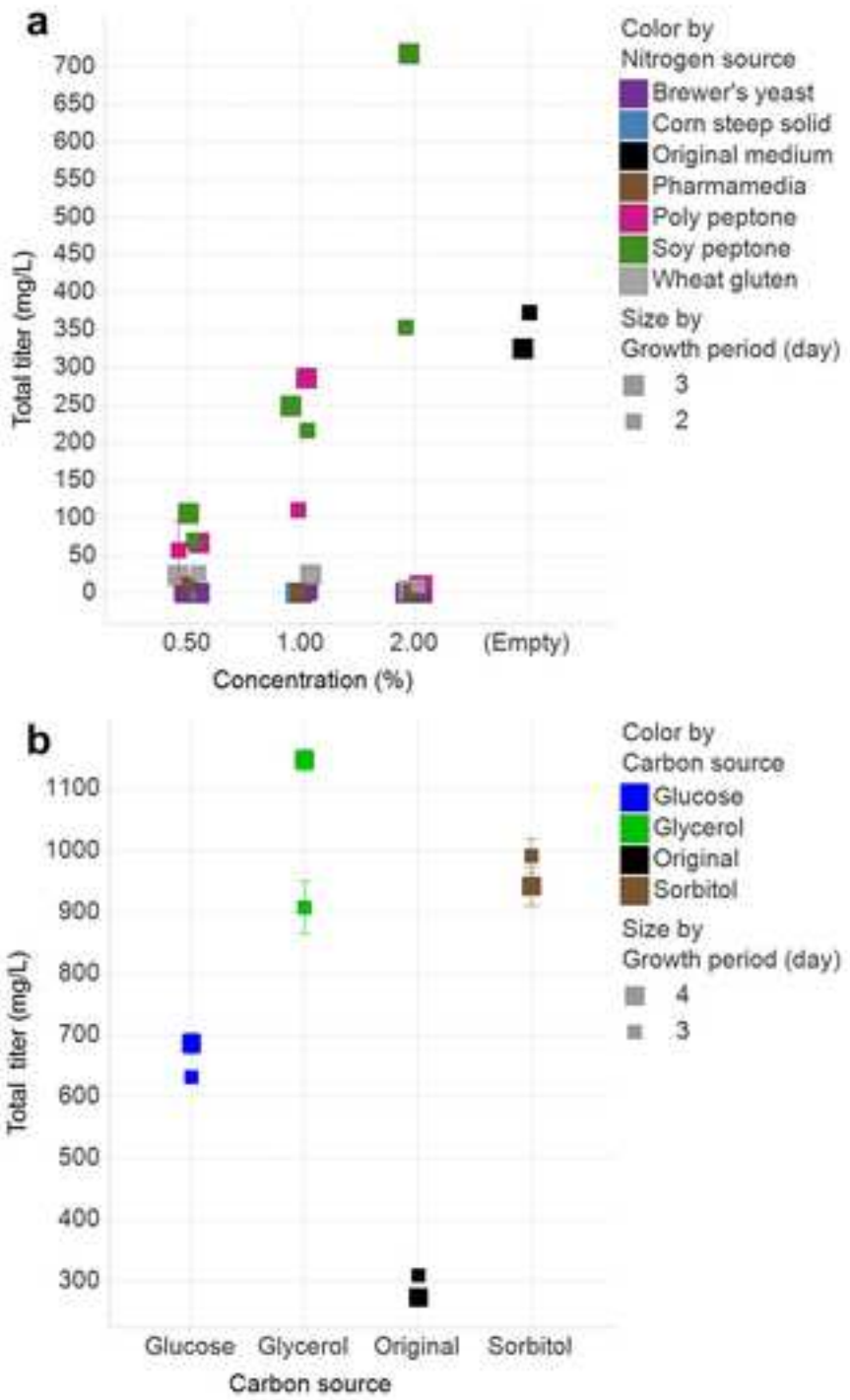

Figure 3

Click here to download high resolution image

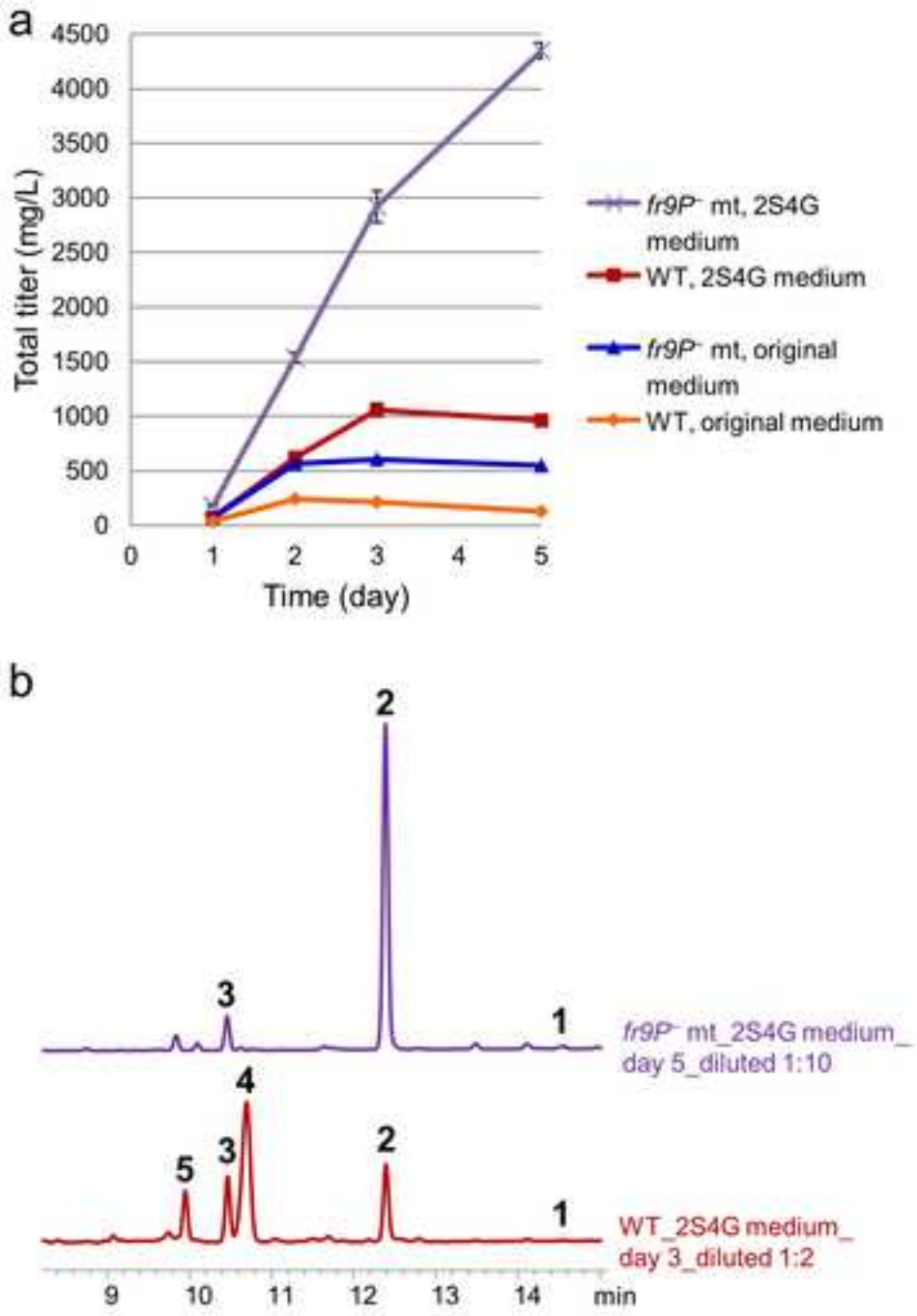

Figure 4

Click here to download high resolution image

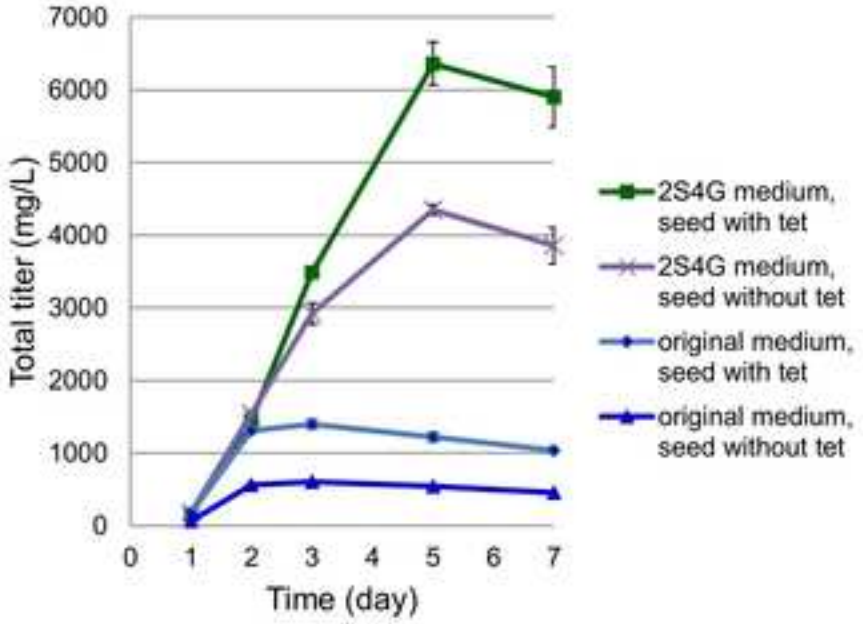

Figure 5

Click here to download high resolution image

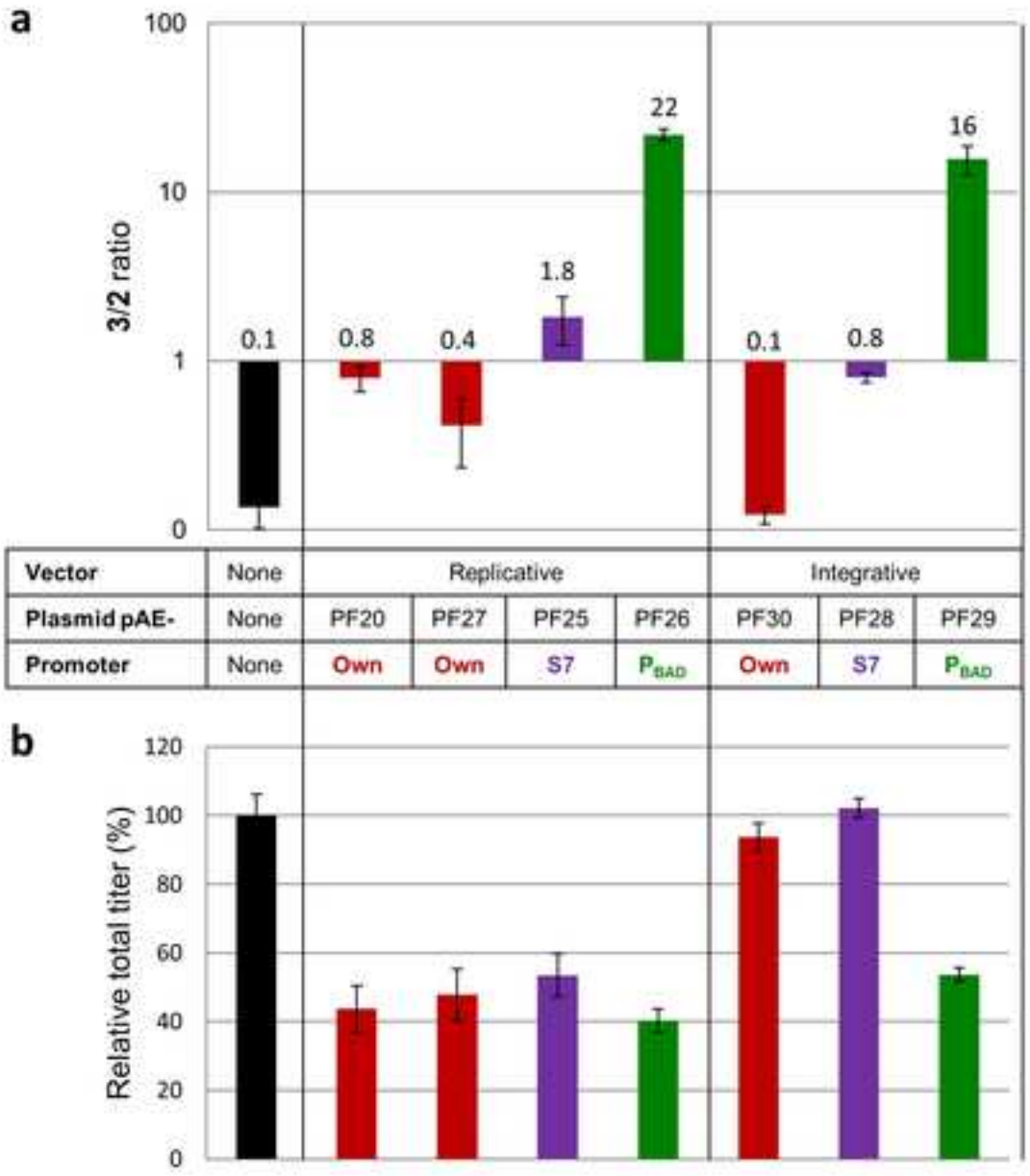

Figure 6

Click here to download high resolution image

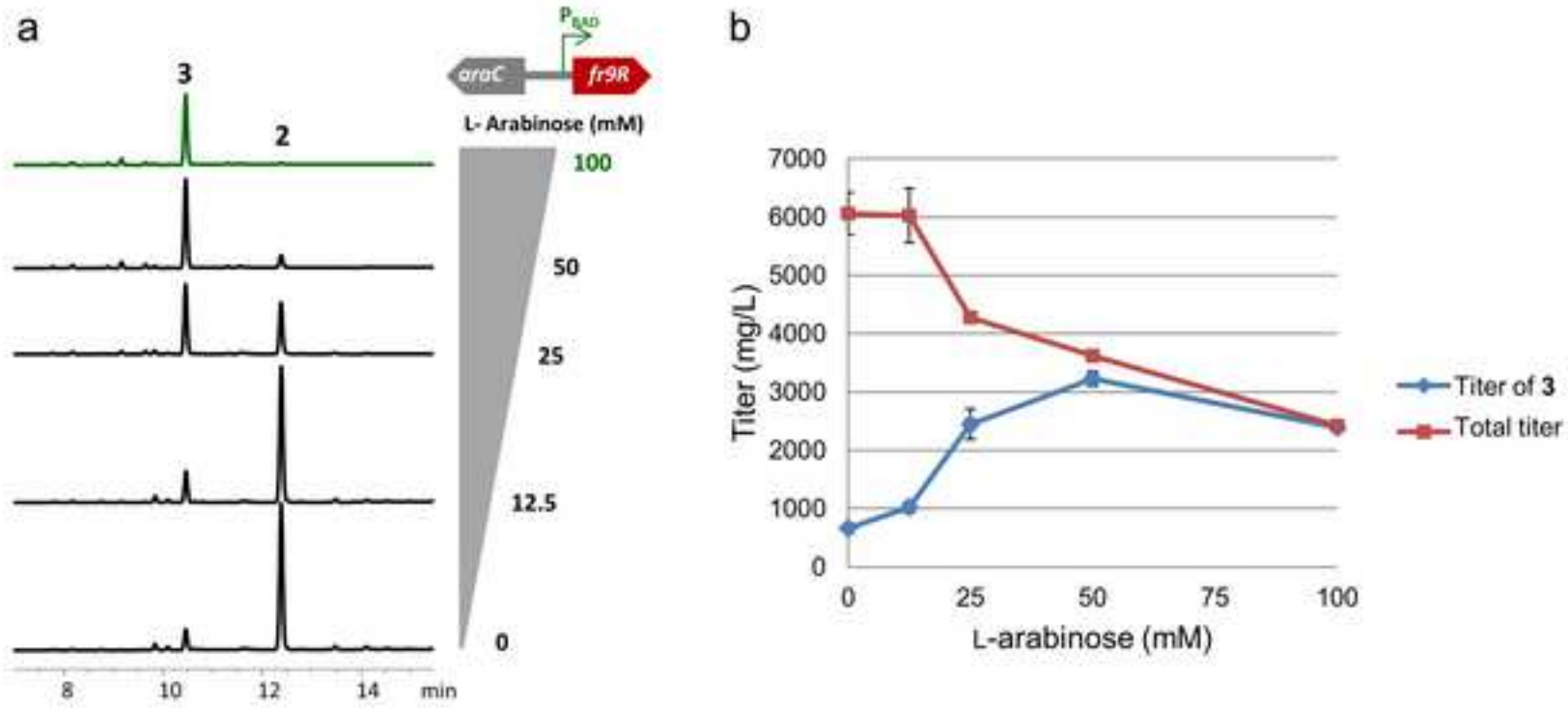

Figure 7

Click here to download high resolution image

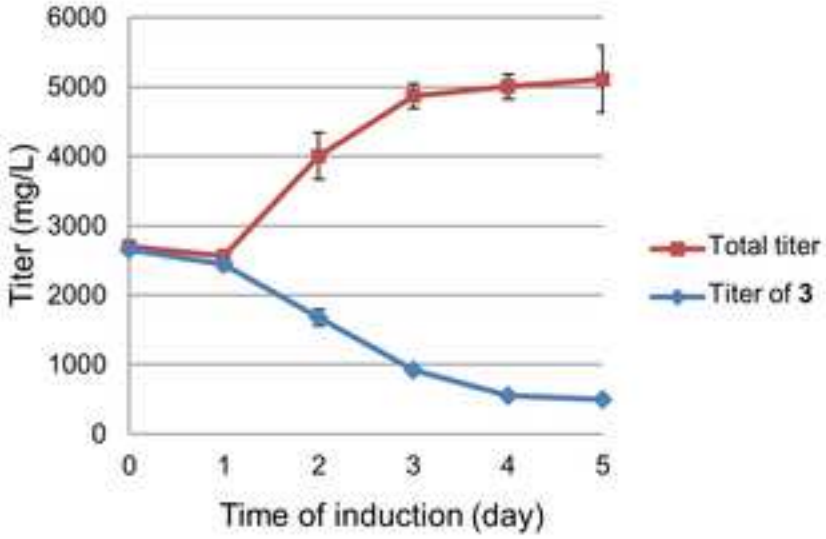

Figure 8

Click here to download high resolution image

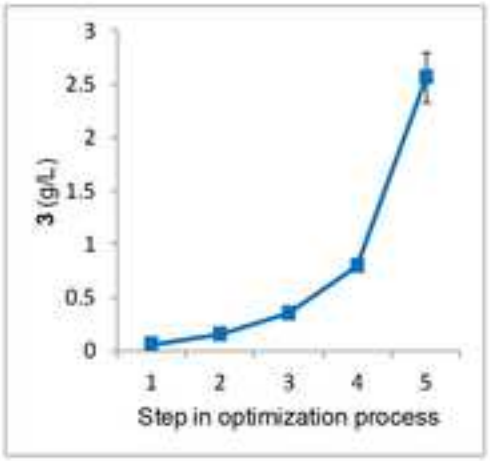

Graphical Abstract

Click here to download high resolution image

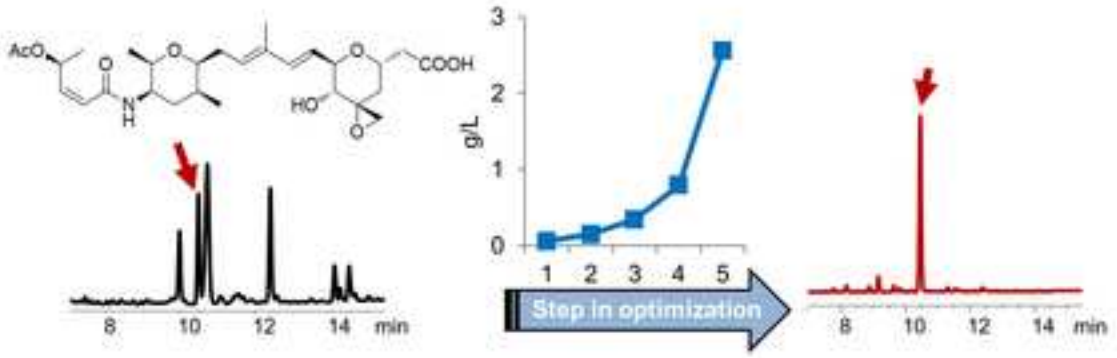

Supplementary Information

Biosynthetic engineering and fermentation media development leads to gram-scale production of spliceostatin natural products in *Burkholderia* sp.

Alessandra S. Eustáquio[1,2]*, Li-Ping Chang[1], Greg L. Steele[1], Christopher J. O'Donnell[1], Frank E. Koehn[1]

[1]Natural Products Laboratory, Worldwide Medicinal Chemistry, Pfizer Worldwide Research and Development, 445 Eastern Point Road, Groton, Connecticut 06340, USA

[2]Present address: University of Illinois at Chicago, College of Pharmacy, Department of Medicinal Chemistry & Pharmacognosy and Center for Pharmaceutical Biotechnology, 900 S Ashland Avenue, Chicago, IL 60607, USA

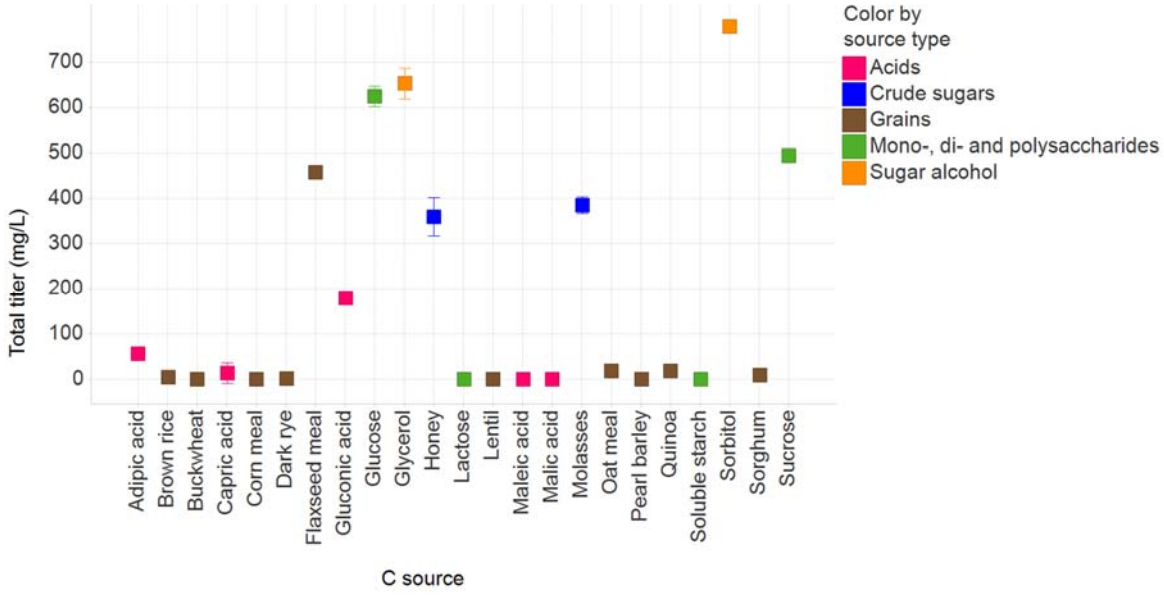

SI Figure 1. Fermentation media development. Effect of carbon source on total spliceostatin production (sum of **1** to **5**). Results shown are average of N=2 ± standard deviation.

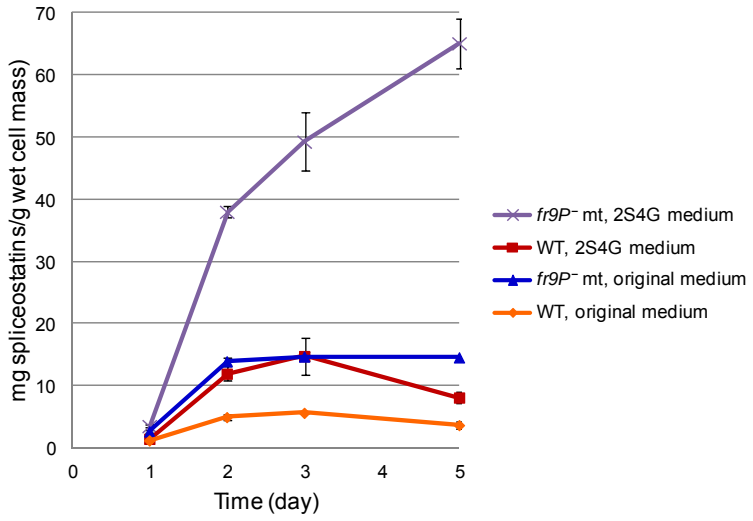

SI Figure 2. **Comparison of metabolite titers produced by *Burkholderia* sp. FERM BP-3421 wild-type and *fr9P*⁻ dioxygenase mutant in original and optimized media normalized by cell mass.** Time-course of total spliceostatins (sum of **1** to **5**) produced by the wild-type (WT) strain per gram wet cell mass in original (orange) and optimized, 2S4G medium (red), and time-course of total spliceostatins (sum of **1** to **3**) produced by the *fr9P*⁻ mutant (mt) strain per gram wet cell mass in original (blue) and optimized, 2S4G medium (purple). Average values of N=3 ± standard deviation.

SI Table 1. 10L Bioreactor fermentation (6% dissolved oxygen) of the *fr9P*$^{-}$ mutant containing pAE-PF29.

Time (h)	Replicate	Titer*: 3 (mg/L)	Titer*: 2 (mg/L)
40	1	393	185
40	2	388	184
64	1	1126	437
64	2	1115	433
68	1	1248	480
68	2	1259	483
72	1	1351	513
72	2	1351	513
88	1	1841	685
88	2	1832	683
92	1	2036	755
92	2	2002	747
96	1	2105	788
96	2	2087	782
112	1	2444	913
112	2	2444	913
116	1	2516	932
116	2	2515	931
Pooled	1	1617	940
Pooled	2	1685	980

*Values correspond to HPLC analysis of culture supernatants, except for the last two lines ("pooled extract") which correspond to HPLC analysis of aliquots from the pooled extract.

SI Table 2. 10L Bioreactor fermentation of the *fr9P*$^{-}$ mutant containing pAE-PF29 at high dissolved oxygen concentrations.

Time (h)	Ferm ID	Replicate	Titer: 3 (mg/L)	Titer: 2 (mg/L)
40	BR1	1	620	145
40	BR2	1	646	112
48	BR1	1	1028	221
48	BR2	1	1055	162
48	CF1	1	889	158
48	CF2	2	963	118
48	CF3	3	973	101
64	BR1	1	1951	352
64	BR2	1	1990	264
70	BR1	1	2132	291
70	BR2	1	2223	207
70	CF1	1	1951	233
70	CF2	2	2113	218
70	CF3	3	2147	182
86	BR1	1	2373	217
86	BR2	1	2425	151
96	CF1	1	2636	113
96	CF2	2	2762	97
96	CF3	3	2689	78
112	CF1	1	2402	51
112	CF2	2	2975	41
112	CF3	3	2725	32

Abbreviations: BR, Bioreactor; CF, Control Flask (2.8L Fernbach flask containing 550 ml medium). BR1, 40% dissolved oxygen. BR2, 60% dissolved oxygen.

SI Table 3. Summary of titer improvement. Titer of **3** and total titers in each step of the optimization process: (1) starting point, i.e. wild-type strain in published medium. (2) wild-type strain in 2S4G medium. (3) *fr9P*$^{-}$ mutant in 2S4G medium. (4) *fr9P*$^{-}$ mutant (seed culture with tetracycline) in 2S4G medium. (5) *fr9P*$^{-}$/pAE-PF29 mutant (seed culture with tetracycline) in 2S4G medium with 100 mM L-arabinose. Average of N≥2 with standard deviation ≤ 10%.

Step	**3** (g/L)	Total (g/L)
1	0.06	0.21
2	0.15	1.06
3	0.35	4.35
4	0.79	6.36
5	2.56	2.6